A Novel Iron(III) Complex with a Tridentate Ligand as a Functional Model for Catechol Dioxygenases: Properties and Reactivity of [Fe(BBA)DBC]ClO_4

Sungho Yoon, Ho-Jin Lee, Kang-Bong Lee,† and Ho G. Jang*

Department of Chemistry and Center for Electro & Photo Responsive Molecules, Korea University, Seoul 136-701, Korea
†Advanced Analysis Center, KIST, Seoul 136-130, Korea
Received May 23, 2000

[Fe^{III}(BBA)DBC]ClO_4 as a new functional model for catechol dioxygenases has been synthesized, where BBA is a bis(benzimidazolyl-2-methyl)amine and DBC is a 3,5-di-*tert*-butylcatecholate dianion. The BBA complex has a structural feature that iron center has a five-coordinate geometry similar to that of catechol dioxygenase-substrate complex. The BBA complex exhibits strong absorption bands at 560 and 820 nm in CH_3CN which are assigned to catecholate to Fe(III) charge transfer transitions. It also exhibits EPR signals at g = 9.3 and 4.3 which are typical values for the high-spin Fe^{III} (S = 5/2) complex with rhombic symmetry. Interestingly, the BBA complex reacts with O_2 within an hour to afford intradiol cleavage (35%) and extradiol cleavage (60%) products. Surprisingly, a green color intermediate is observed during the oxygenation process of the BBA complex in CH_3CN. This green intermediate shows a broad isotropic EPR signal at g = 2.0. Based on the variable temperature EPR study, this isotropic signal might be originated from the [Fe(III)-peroxo-catecholate] species having low-spin Fe^{III} center, not from the simple organic radical. Consequently, it allows O_2 to bind to iron center forming the Fe(III)-superoxide species that converts to the Fe(III)-peroxide intermediate. These present data can lead us to suggest that the oxygen activation mechanism take place for the oxidative cleaving catechols of the five-coordinate model systems for catechol dioxygenases.

Introduction

The catechol dioxygenases are non-heme iron-containing enzymes that play key roles in the metabolism of various aromatic compounds, converting aromatic pollutants to aliphatic products by the oxidative ring cleavage in the environment.[1] They are found in soil bacteria and subdivided into two different classes.[2] The first one is the intradiol-cleaving enzymes containing Fe(III) center that catalyze a C_1-C_2 bond cleavage giving muconic acids and the second one is the extradiol-cleaving enzymes containing Fe(II) that catalyze either a C_2-C_3 or C_1-C_6 bond cleavage giving muconic semialdehyde (Scheme 1).

There has been a significant progress[3-8] toward understanding the structure of the active site and reaction mechanism of the intradiol-cleaving enzymes. It was highlighted by the crystal structure of native protocatechuate 3,4-dioxygenase (3,4-PCD) showing that the Fe(III) center of the 3,4-PCD enzyme has five-coordinate geometry.[9] Furthermore, recent crystallographic studies prove that the Fe(III) center remains as a five-coordinate geometry even after binding the catechol substrate.[10,11] Model systems that mimic enzymatic reactions are important mechanistic tools, because the flexibility in ligand design allows a systematic investigation of the important factors affecting reactivity as well as reaction mechanism.[12-17] However, most of the previous Fe(III)-catecholato complexes have six-coordinated metal center with tetradentate ligands. Even though they suggest some aspects of the intradiol-cleaving mechanism, they do not provide any direct evidence for the real entity of the active species in the oxygenation and reaction mechanism. Recently, five-coordinate Fe(III)-catecholato complexes with the TACN and Tp^R ligand are the only known examples of complexes with a facial-capping tridentate ligand.[18-20] [Fe^{III}(TACN)DBC] that was prepared by treating with [Fe^{III}(TACN)DBC(Cl)] with $AgNO_3$ and base gave only extradiol cleavage products near quantitatively.[18] However, [Fe^{III}($Tp^{i\text{-}Pr2}$)DBC] gives a mixture of intradiol and extradiol cleavage products, which is quite different pattern from the TACN complex.[19]

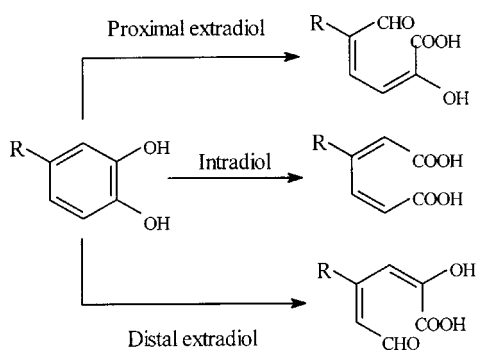

Scheme 1

In this paper, we report the synthesis and spectroscopic properties of the five-coordinate [Fe^{III}(BBA)DBC]ClO_4 complex as a structural and functional model for catechol dioxygenases. One vacant coordination site of the metal center in the BBA complex give a profound influence on the selectivity of dioxygen attack and the stability of the possible Fe(III)-peroxo intermediate during the oxygenation pro-

cess. We discuss the possible intermediate and propose the new oxygenation mechanism of the five-coordinate model systems for the catechol dioxygenases.

Experimental Section

All reagents and solvents were purchased from commercial sources and used as received, unless noted otherwise. CH_3CN was distilled from CaH_2 under nitrogen before use. $DBCH_2$ was purified by the recrystallization from hexane.[21] $DBCH_2$-4,6-d_2 was prepared by deuterium exchange in D_2O in the presence of a substoichiometric amount of base at 140 °C in a sealed tube for ~4 hours.[21] Microanalysis was performed by Korean Basic Science Research Institute, Seoul.

Synthesis of Bis(benzimidazolyl-2-methyl)amine, **BBA**. Iminodiacetic acid (13.3 g, 0.1 mol) and 1,2-diaminobenzene (20.2 g, 0.2 mol) were mixed and heated to 180 °C-200 °C until no further steam was evolved. It was allowed to cool to room temperature. The dark glassy solid was taken up in hot hydrochloric acid (4 M, 200 mL) and filtered. After cooling the trihydrochloride salt of BBA, a pale blue feathery solid was obtained. This was taken up in warm water (200 mL) with KOH (28.0 g, 0.5 mol), and the solution was refluxed for 30 min. Methanol was added until the precipitate redissolved. After refluxing with charcoal as a decolorizing agent (15 min), the solution was filtered and obtained the crude free amine product upon cooling. Two times of recrystallization from methanol-water gave BBA · H_2O as white needles. (25% yield) mp.: 270 °C (decomp.), ^{1}H NMR (300 MHz, d_6-DMSO) δ 7.52 (m, 4H, aryl H), 7.19 (m, 4H, aryl H), and 4.09 (s, 4H, CH_2).

Synthesis of [Fe^{III}(BBA)DBC]ClO$_4$. [Fe^{III}(BBA)DBC]ClO_4 was synthesized by mixing 448 mg (1.52 mmol) BBA · H_2O and 783 mg (1.52 mmol) $Fe(ClO_4)_3 \cdot 9H_2O$ in 10 mL methanol under argon. After 30 minute reaction time, 337 mg (1.52 mmol) $DBCH_2$ and Et_3N 0.528 mL (3.8 mmol) was added slowly under argon. After 1 hr, the purple solution was filtered and dried under vacuum. The crude purple-blue powder was obtained and stored in the glove box. The pure complex was obtained by the recrystallization from the methanol solution of the crude product. FAB$^+$-Mass m/z: 553. Anal. Calcd. for [Fe(BBA)DBC]ClO_4, $C_{30}H_{35}FeN_5O_2Cl$: C, 55.19; H, 5.40; N, 10.73. Found: C, 55.36; H, 5.53; N, 10.87.

Caution ! While the present perchlorate complex is not explosive, care is recommended.

Physical Methods. UV-visible spectra were obtained on a Hewlett-Packard 8453 biochemical analysis spectrophotometer. IR spectra were obtained Bomem 102 FT-IR spectrometer. Standard organic product analyses were performed using a Hewlett-Packard 6890 Series plus Gas Chromatograph equipped with a flame ionization detector or a reverse-phase isocractic HPLC (Waters 600E with tunable absorbance detector and C18 column). ^{1}H NMR spectra were obtained on a Varian VXR 300 spectrometer.

Characterization of Oxygenation Products. The four major organic products of the [Fe(BBA)DBC]$^+$ were identified by using GC, GC-Mass, HPLC, IR, and NMR spectroscopy. Spectroscopic data are as follows:

3,5-di-*tert*-butyl-5-(carboxymethyl)-2-furanone (**1**): IR (KBr) ν_{CO} 1755, 1723 cm^{-1}, $\nu_{C=C}$ 1644 cm^{-1}; ^{1}H NMR ($CDCl_3$): 0.96 (s, 9H), 1.21 (s, 9H), [2.74, 2.81, 2.91, 2.98 (AB q, J_{AB} = 14 Hz, 2H)], 6.93 (s, 1H), 9.70 (s); ^{13}C NMR ($CDCl_3$): 24.9 (q), 27.6 (q), 31.2 (s), 37.1 (t), 37.4 (s), 87.8 (s), 143.6 (s), 145.2 (d), 170.9 (s), 174.7 (s).

3,5-di-*tert*-butyl-1-oxacyclohepta-3,5-diene-2,7-dione (**2**): IR (KBr) ν_{CO} 1783, 1741 cm^{-1}, $\nu_{C=C}$ 1636, 1600 cm^{-1}; ^{1}H NMR ($CDCl_3$): 1.16 (s, 9H), 1.28 (s, 9H), 6.14 (d, J = 2 Hz, 1H), 6.45 (d, J = 2 Hz, 1H); ^{13}C NMR ($CDCl_3$): 28.4 (q), 28.9 (q), 36.2 (s), 36.5 (s), 115.5 (d), 123.9 (d), 148.0 (s), 160.0 (s), 162 (s).

3,5-di-*tert*-butyl-2-pyrone (**3**): IR (KBr) ν_{CO} 1710 cm^{-1}, $\nu_{C=C}$ 1635, 1560 cm^{-1}; ^{1}H NMR ($CDCl_3$): 1.20 (s, 9H), 1.32 (s, 9H), 7.04 (d, 1H), 7.14 (d, 1H); ^{13}C NMR ($CDCl_3$): 28.4 (q), 29.5 (q), 31.9 (s), 34.8 (s), 127.4 (s), 136.2 (s), 136.3 (s), 143.8 (d), 160.9 (s).

4,6-di-*tert*-butyl-2-pyrone (**4**): IR (KBr) ν_{CO} 1710 cm^{-1}, $\nu_{C=C}$ 1630, 1550 cm^{-1}; ^{1}H NMR ($CDCl_3$): 1.19 (s, 9H), 1.26 (s, 9H), 6.01 (d, 2H); ^{13}C NMR ($CDCl_3$): 28.1 (q), 29.0 (q), 35.5 (s), 36.2 (s), 98.7 (s), 107.2 (s), 163.4 (d), 167.7 (d), 171.4 (s).

Oxygenation Studies. Reactivity studies were performed in organic solvents in an oxygen atmosphere under ambient conditions. After the reaction was complete, as indicated by the loss of color, the solution was concentrated under reduced pressure. The organic products were extracted with ether, dried over anhydrous Na_2SO_4, and then concentrated. The remaining residue was dissolved in CH_3CN and acidified with HCl to pH 3 to decompose the [μ-oxo-diiron(III)(BBA)$_2$] complex. The furanone acid was extracted with ether, dried, and concentrated. The extracts were then subjected to GC or reverse-phase isocractic HPLC separation (conditions are same as previously reported in reference 14).

Oxygenation studies were performed on a HP-8453 diode array spectrometer with temperature control by an Endocal RTE-5 refrigerated circulation bath. Oxygen was bubbled through the solution (0.5-0.8 mM in complex) and then maintained at 1 atm of pressure above the reacting solution.

Results and Discussion

Spectroscopic and Electrochemical Properties. [Fe^{III}(BBA)DBC]ClO_4 is an air-sensitive puple-blue complex that exhibits two intense absorption bands at 560 and 820 nm (ε = 1670, 2050 M^{-1}cm^{-1}, respectively) in CH_3CN (Figure 1). These bands are assigned to the catecholate to Fe(III) charge transfer bands based on the extinction coefficient, spectral shifts with various substituted catechols, and the comparison with known [Fe^{III}(L)DBC] complexes.[12-17] These values are quite red-shifted than [Fe^{III}(TACN)(DBC)]$^+$ complex (444 and 695 nm), but blue-shifted than [Fe^{III}(Tp$^{i\text{-}Pr2}$)DBC] complex (574 and 1046 nm).[18,19] The redox wave for BBA complex in DMF shows ε^o value (432 mV *vs* SCE) for the Fe(III)DBSQ/Fe(III)DBC couple. This is considerably

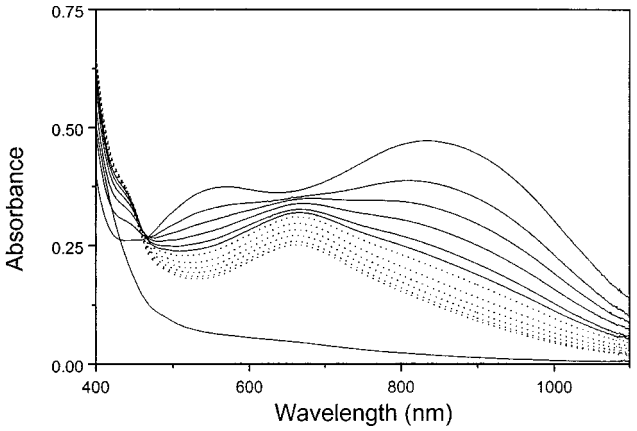

Figure 1. Oxygenation process of the reaction of [Fe(BBA)-DBC]ClO_4 in CD_3CN with O_2 as monitored by disappearance of catecholate to Fe^{III} charge transfer bands at 20 °C. The dotted lines represent the formation and decay of the green intermediate.

more positive than the free DBC/DBSQ couple value.[22] This large positive shift indicates that the DBC oxidation state is stabilized upon the interaction with the Fe^{III}. Furthermore, this redox potential is more positive than that of $[Fe^{III}$-(TACN)(DBC)$]^+$ (310 mV) and $[Fe^{III}(Tp^{i\text{-}Pr2})$DBC] (100 mV), reflecting that the BBA complex has more Lewis acidic Fe^{III} center.

NMR Properties. The $[Fe^{III}$(L)DBC] complexes exhibit large NMR contact shifts, which provide some information regarding the electronic structure of the paramagnetic complexes.[23] The NMR spectrum of BBA complex suggests that this complex has a high-spin Fe(III) center due to the broad line-width and large chemical shifts (Figure 2). Very surprisingly, the total numbers of peaks are well matched with the asymmetric ligand environment around the metal center. In other words, the BBA ligand loses the 2-fold symmetry in the solution. This presumably arises from the rigidity of the $[Fe^{3+}$(BBA)DBC]ClO_4 complex, which enforced by the DBC. The peak assignments are based on the integration, the comparison with the selective deuterated complexes, and T_1 measurement. The meta and para protons of benzimidazolyl moiety dominate the NMR spectrum of BBA complex. Four meta protons appear as relatively sharp features at 30 and -9.5 ppm, and -8.5 and -30 ppm with T_1 values of 11 and 12 ms, and 6.3 and 6.9 ms, respectively. Two para protons appear at 3.5 and 2.9 ppm with T_1 values of 67 and 76 ms, respectively. These peaks were confirmed by the connectivity observed in COSY spectrum as shown in Figure 3. While two ortho protons are observed at 48 and 52 ppm with T_1 values of 2.1 and 1.9 ms, respectively. Additional peaks arise from the methylene protons (H_b, H_c) that appear as broad bands at 75 and 48 ppm with T_1 value of 0.3 ms. Proton of the secondary amine (N-H_a) was observed as a very broad peak at 93 ppm due to the close proximity from the metal center. Protons of the imidazole ring (N-H_d) appear at 35 and -18 ppm that are confirmed by the comparison with the methyl substituent one. Furthermore, the DBC-5-*t*-butyl and 3-*t*-butyl proton resonances are quite downfield shifted at 7.6 and 4.6 ppm due to their coordination to the Fe(III) center. To assign the other catecholate protons, ^{1}H NMR spectrum of $[Fe^{3+}$(BBA)DBC-4,6-d_2]ClO_4 complex reveals that the 4-H of the catecholate appears at quite upfield region (-47 ppm). The variable temperature NMR study was performed to investigate the possible semiquinone character of the didentate catecholate. When δ is plotted *vs.* 1/T, the peaks from the benzimidazolyl moiety converge to the diamagnetic region at very high temperature according to the Curie law.[24] However, the 4-H proton of the DBC does not converge to the diamagnetic region, but stays at -47 ppm (Figure 4). Thus, we can suggest that there is a strong paramagnetic property in the catechol ring. This result is proba-

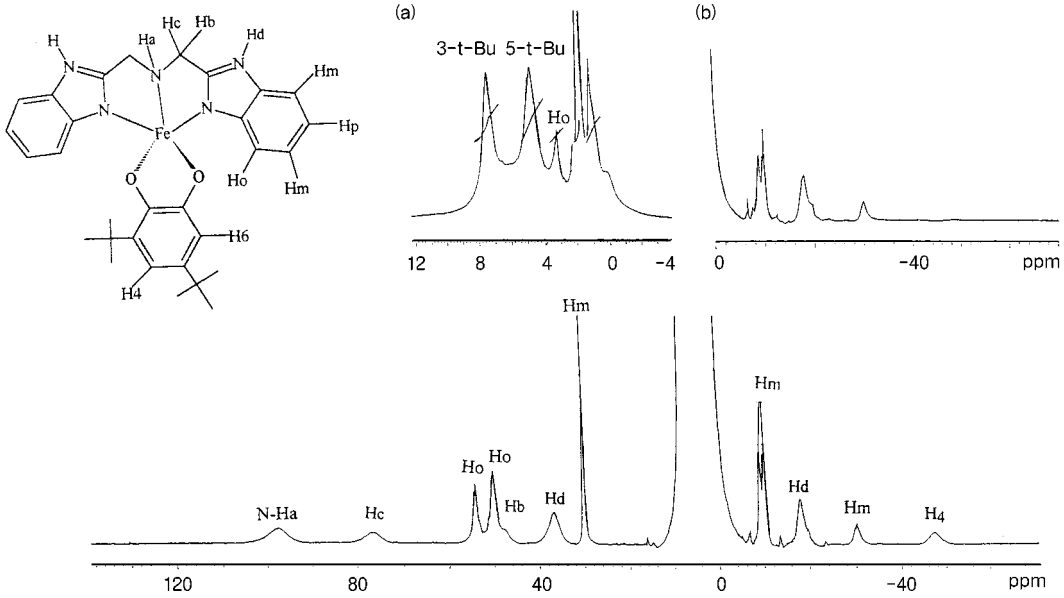

Figure 2. ^{1}H NMR spectrum of [Fe(BBA)DBC]ClO_4 in CD_3CN under argon with ambient conditions. (a) The right inset is an expansion of diamagnetic region of the main spectrum. (b) The left inset is the spectrum of [Fe(BBA)DBC-4,6-d_2]ClO_4.

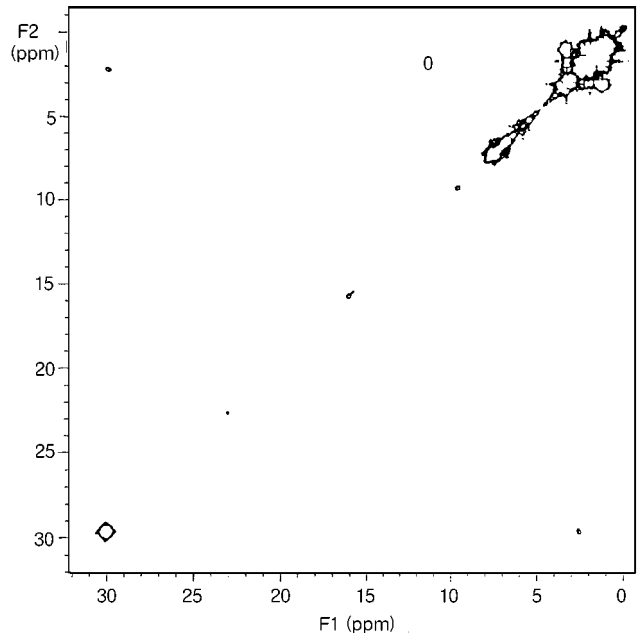

Figure 3. COSY spectrum of [Fe(BBA)DBC]ClO_4 in CD_3CN under argon.

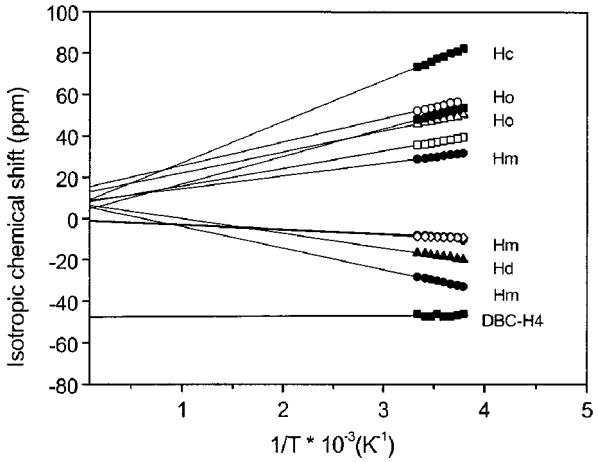

Figure 4. Plot of chemical shift (δ) *vs.* 1/Temperature (1/K) of [Fe(BBA)DBC]ClO_4 in CD_3CN under argon.

bly due to the [Fe(II)-DBSQ] character in [Fe(III)-DBC] complex due to the enhanced covalency of the metal-catecholate interaction.[15] Also, this [Fe(II)-DBSQ] character makes it possible to observe the relative sharp signals in ^{1}H NMR spectrum compared with other high-spin Fe(III) complexes.[14] After the complete oxygenation, NMR spectrum of the complex shows very broad and almost diamagnetic pattern that is typical for the formation of μ-oxo-diiron(III) complex due to the strong *antiferromagnetic* coupling interaction between the high-spin iron(III) centers (refer to EPR section).

Oxygenation Process and EPR Properties. EPR spectrum of the BBA complex exhibits signals at g = 9.3 and 4.3 at 4 K corresponding to the ground and middle Kramers doublets of the typical high-spin Fe^{III} (S = 5/2) with rhombic symmetry (Figure 5).[25] A weak signal at g = 2.0 arises from the minor species with S = 1/2 system, presumably arising

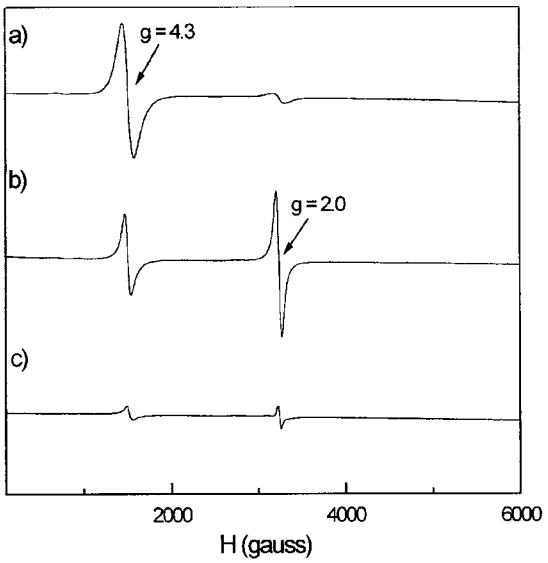

Figure 5. X-band EPR spectra: a) [Fe(BBA)DBC]ClO_4 in CH_3CN under argon. b) green intermediate after the exposure to O_2 for a few minutes. c) [Fe(BBA)DBC]ClO_4 in CH_3CN after the complete oxygenation. Spectra were obtained at 9.22 GHz with 100 kHz modulation at 4 K.

from the low-spin Fe^{III} species. When the CH_3CN solution of BBA complex was exposed to O_2, its characteristic purple-blue color (λ = 560 nm) immediately changes to green color intermediate (λ = 660 nm) and gradually turns to yellow oxygenated compound as shown in Figure 1. Even though we have not succeed to stabilize and isolate the green intermediate at low temperature due to its intrinsic instability, we can get an EPR spectrum of the green intermediate showing a broad isotropic signal at g = 2.0 with 60 G line-width. This signal may come from either organic radical or low-spin Fe^{III} center. In order to investigate the origin of this signal, we performed the variable temperatures EPR study (Figure 6). If the signal were originated from the low-spin Fe^{III} center, it will decrease dramatically as the temperature increase due to the Boltzman population of the spin state. In fact, the signal at g = 2.0 decrease sharply as the temperature increase. Thus,

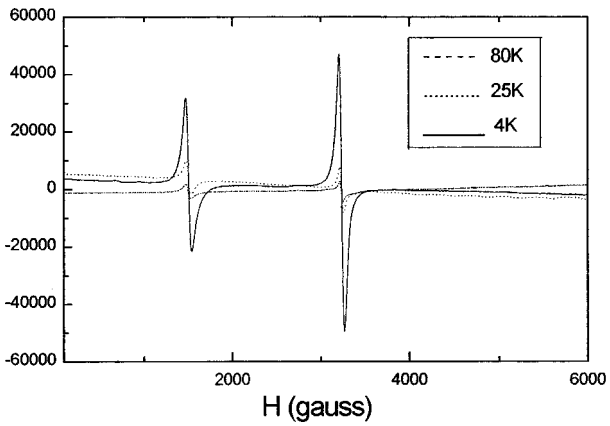

Figure 6. Variable temperature X-band EPR spectra of the green intermediate.

we can suggest that BBA complex undergoes oxygenation process *via* low-spin Fe^{III} intermediate (probably [Fe(III)-peroxide species). After the complete oxygenation, the EPR spectrum at 4K does not show any significant EPR signals except very weak signals at g = 4.3 and 2.0. In other words, the BBA complex makes μ-oxo diiron(III) complex which is EPR silent due to the *antiferromagnetic* coupling between the iron(III) centers (S = 0) which is quite well matched with NMR data.

Reactivity and Reaction Mechanism. The [Fe^{III}(L)DBC] complexes react with dioxygen to yield products due to the oxidative cleavage of the catechol ring.[12-16] Kinetic studies of the reaction of the BBA complex with 1 atm O_2 in CH_3CN under pseudo-first order conditions show that the BBA complex reacts very fast with O_2. However, the measurement of the reaction rate is meaningless since the green intermediate was growing during the oxygenation process. The BBA complex reacts with O_2 within an hour to afford intradiol and extradiol cleavage products as shown in Scheme 2. The oxygenated products are intradiol cleavage product (3,5-di-tert-butyl-oxacyclohepta-3,5-diene-2,7-dione (**1**), 35%) and extradiol cleavage products (3,5-di-*tert*-butyl-2-pyrone (**3**), 28% and 4,6-di-tert-butyl-2-pyrone (**4**), 32%). This is probably due to the availability of a vacant coordination site on the Fe(III) center that allows O_2 bind to iron center and facilitate its attack on the catecholate to afford intradiol and extradiol cleavage products. This result is quite different from those of five-coordinate complexes [Fe^{III}-(TACN)(DBC)]$^+$ (only extradiol cleavage product, 35%)[18] and [Fe^{III}($Tp^{t\text{-}Bu,i\text{-}Pr}$)DBC] (no oxygenated product).[19] But, it is quite similar to the result of the pseudo six-coordinated [Fe^{III}(Tp^{iPr2})DBC · (CN_3CN)] giving intradiol (**1**, 33%) and extradiol cleavage products (**3**, 28% and **4**, 39%).[19]

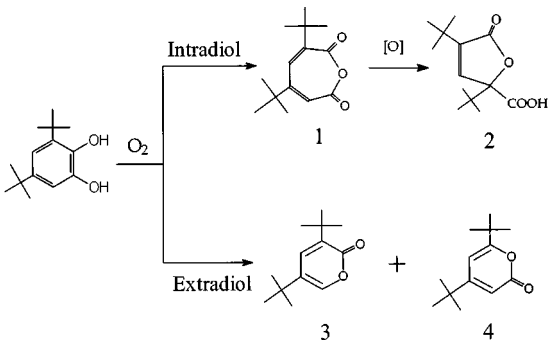

Scheme 2

Together with oxygenation pattern and oxygenated product, we can suggest a possible reaction mechanism for the the oxygenation of the BBA complex as shown in Scheme 3. First of all, the semiquinone character in the BBA complex has been suggested by the low energy charge transfer band as well as variable temperature NMR study. The Fe(II) character of the Fe(II)-DBSQ facilitates the attack of O_2 at the vacant coordination site of Fe(II)-DBSQ, generating a [superoxide-Fe^{III}-DBSQ] complex. This is in good agreement with the suggested oxygen activation mechanism of the [Fe^{III}(TACN)DBC]$^+$ system which only yield extradiol cleavage products.[17] This superoxide then couples with the DBSQ radical forming the [peroxide-Fe^{III}-DBSQ] intermediate that is analog to the recently isolated and characterized as a [Ir-peroxo-$(PPh_3)_3$DBC] by Bianchini *et al*.[26] Therefore, the extradiol cleavage products might be originated from the direct attack of O_2 to Fe(II) center that makes the Fe(II)-O_2^- species and converted to peroxy intermediate during the oxygenation process.[17,27]

Unfortunately, it is impossible at this point to determine whether all starting complex reacts with dioxygen *via* only green color intermediate or not. Thus, we cannot exclude the substrate activation mechanism[28] that might be involved in the intradiol cleavage of catechol, in which O_2 attack on the coordinated catecholate. A peroxide complex is proposed to form subsequently to O_2 binding and then decompose to the intradiol cleavage products. Therefore, we can suggest that the BBA complex can undergo two different oxygenation pathways (Scheme 3). The major pathway involves the direct attack of O_2 to Fe(II) center, forming the Fe^{III}-superoxide species that presumably gives the extradiol cleavage product and the minor pathway might take the substrate activation mechanism during the oxygenation process giving intradiol cleavage products.

In summary, a five-coordinate [Fe(BBA)DBC] complex has been prepared as a new functional model for catechol dioxygenases. Importantly, we can observe the green color intermediate with EPR and UV/visible spectroscopy during the oxygenation process. In addition, it is very important to emphasize that the intradiol and extradiol cleavage products

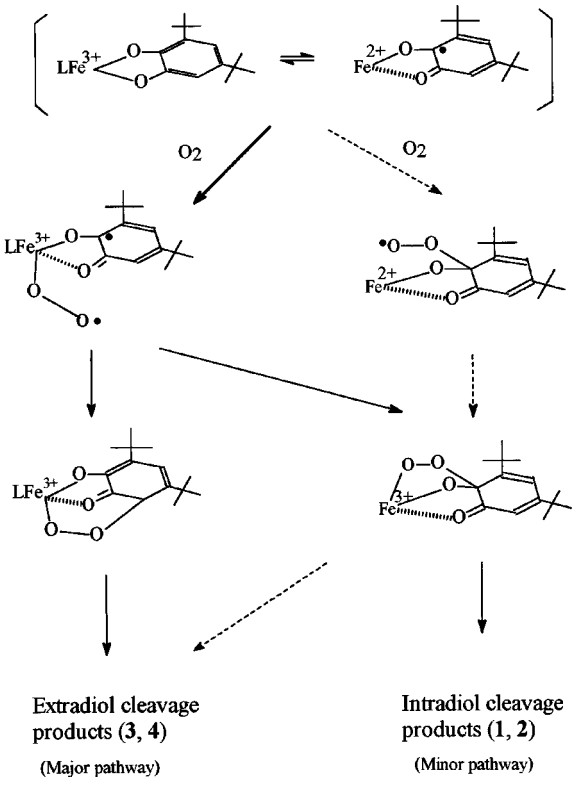

Scheme 3

are observed for the oxygenation of five-coordinate BBA complex. This is probably due to the fact that the benzyl substituent of the BBA ligand does interfere and control the oxygenation pathway similar to the effect of the hydrophobic pocket around the metal center in the real enzyme-substrate system. This result can provide an important idea how to control the selectivity between intradiol and extradiol cleavage products. Consequently, the steric effect around the metal center can be more crucial than the simple electronic effect of the metal center in the five-coordinate model systems. In order to isolate and identify the intermediate and elucidate the exact oxygenation mechanism of the CTD-substrate complex, five coordinate model complexes with bulky and hydrophobic ligand are needed.

Acknowledgment. This research was supported by CRM-KOSEF (2000) and Brain Korea 21 Program.

References

1. (a) Reineke, W.; Knackmuss, M. J. *Ann. Rev. Microbiol.* **1988**, *42*, 263. (b) Dekkar, M. In *Microbial Degradation of Organic Molecules*; Gibson, D. T., Ed.; New York, 1984.
2. (a) Que, L., Jr. *J. Chem. Educ.* **1985**, *62*, 938. (b) Que, L., Jr. In *Iron Carriers and Iron Proteins*; Loehr, T. M., Ed.; VCH Publishers: New York, 1989; p 467. (c) Que, L., Jr.; Ho, R. Y. N. In *Dioxygen Activation by Enzymes with Mononuclear Iron Active Sites*, *Chem. Rev.* **1996**, *96*, 2607.
3. Kent, T. A.; Münck, E.; Pyrz, J. W.; Widom, J.; Que, L., Jr. *Inorg. Chem.* **1987**, *26*, 1402.
4. (a) Que, L., Jr.; Heistand, R. H., II; Mayer, R.; Roe, A. L. *Biochemistry* **1980**, *19*, 2588. (b) Que, L., Jr.; Epstein. R. M. *Biochemistry* **1981**, *20*, 2545.
5. Whittaker, J. W.; Lipscomb, J. D. *J. Biol. Chem*. **1984**, *259*, 4487.
6. Felton, R. H.; Barrow, W. L.; May, S. W.; Sowell, A. L.; Goel, S. *J. Am. Chem. Soc.* **1982**, *104*, 6132.
7. Que, L., Jr.; Lauffer, R. B.; Lynch, J. B.; Murch, B. P.; Pyrz, J. W. *J. Am. Chem. Soc*. **1987**, *109*, 5381.
8. (a) Bull, C.; Ballou, D. P.; Otsuka, S. *J. Biol. Chem*. **1981**, *256*, 12681. (b) Walsh, T. A.; Ballou, D. P.; Mayer, R.; Que, L., Jr. *J. Biol. Chem*. **1983**, *258*, 14422.
9. (a) Ohlendorf, D. H.; Lipscomb, J. D.; Weber, P. C. *Nature* **1988**, *336*, 403. (b) Ohlendorf, D. H.; Orville, A. M.; Lipscomb, J. D. *J. Mol. Biol.* **1994**, *244*, 586.
10. (a) Whittaker, J. W.; Lipscomb, J. D.; Kent, T. A.; Munck, E.; Orme-Johnson, N. R.; Orme-Johnson, W. H. *J. Biol. Chem*. **1984**, *259*, 4466. (b) Orville, A. M.; Lipscomb, J. D. *J. Biol. Chem*. **1989**, *264*, 8791. (c) True, A. E.; Orville, A. M.; Pearce, L. L.; Lipscomb, J. D.; Que, L., Jr. *Biochemistry* **1990**, *29*, 10847.
11. Orville, A. M.; Lipscomb, J. D.; Ohlendorf, D. H. *Biochemistry* **1997**, *36*, 10052.
12. Que, L., Jr.; Kolanczyk, R. C.; White, L. S. *J. Am. Chem. Soc*. **1987**, *109*, 5373.
13. Cox, D. D.; Benkovic, S. J.; Bloom, L. M.; Bradley, F. C.; Nelson, M. J.; Que, L., Jr.; Wallick, D. E. *J. Am. Chem. Soc*. **1988**, *110*, 2026.
14. Cox, D. D.; Que, L., Jr. *J. Am. Chem. Soc.* **1988**, *110*, 8085.
15. Jang, H. G.; Cox, D. D.; Que, L., Jr. *J. Am. Chem. Soc.* **1991**, *113*, 9200.
16. Koch, W. O.; Krüger, H.-J. *Angew. Chem. Int. Ed. Engl.* **1995**, *34*, 2671.
17. Lim, J. H.; Lee, H.-J.; Lee, K.-B.; Jang, H. G. *Bull. Korean Chem. Soc*. **1997**, *18*, 1166.
18. Ito, M.; Que, L., Jr. *Angew. Chem., Int. Ed. Engl.* **1997**, *36*, 1342.
19. Ogihara, T.; Moro-oka, Y. *Inorg. Chem*. **1998**, *37*, 2614.
20. Abbreviations: $DBCH_2$, 3,5-di-tert-butylcatechol; TACN, triazacyclononane; BPLA is bis(2-pyridylmethyl)(6-methyl-2-pyridylmethyl)amine. $Tp^{t\text{-}Bu,i\text{-}Pr}$ is hydrotris(3-tert-butyl-5-isopropyl-pyrazolyl)borate, $Tp^{i\text{-}pr2}$, hydrotris(3,5-di-isopropyl-pyrazolyl)borate.
21. Pyrz, J. W.; Roe, A. L.; Stern, L. J.; Que, L., Jr. *J. Am. Chem. Soc*. **1985**, *107*, 614.
22. Nanni, E. J., Jr.; Stallings, M. D.; Sawyers, D. T. *J. Am. Chem. Soc*. **1980**, *102*, 4481.
23. Bertini, I.; Luchinat, C. *NMR of Paramagnetic Molecules in Biological Systems*; The Benjamin/Cummings Publishing Company Inc.: California, 1986.
24. Wu, F.; Kurtz, Jr. D. M. *J. Am. Chem. Soc.* **1989**, *111*, 6563.
25. Wertz, J. E.; Bolton, J. R. *Electron Spin Resonance; Elementary Theory and Practical Application*; Chapman and Hall: New York, 1986.
26. Barbaro, P.; Bianchini, C.; Mealli, C.; Meli, A. *J. Am. Chem. Soc*. **1991**, *113*, 3181.
27. Funabiki, T.; Mizoguchi, A.; Sugimoto, T.; Tada, S.; Tsuji, M.; Yoshioka, T.; Sakamoto, H.; Takano, M.; Yoshida, S. *J. Am. Chem. Soc*. **1986**, *108*, 2921.
28. Que, L., Jr.; Lipscomb, J. D.; Münck, E.; Wood, J. M. *Biochim. Biophys. Acta* **1977**, *485*, 60.